Research Square

Preprints are preliminary reports that have not undergone peer review.
They should not be considered conclusive, used to inform clinical practice,
or referenced by the media as validated information.

Radiation simulation of ^{60}Fe in lunar regolith decay

Zheng yang Pei
Xizang University
Hua Bao
1120710608@qq.com
Xizang University
Zi yi Wang
Xizang University
Zhi Li
Xizang Museum of Natural Science

Research Article

Keywords: 60Fe, Lunar regolith, γ-ray radiation transmission, Mass absorption coefficient, Flux, Sensitivity threshold

Posted Date: October 27th, 2026

DOI: https://doi.org/10.21203/rs.3.rs-11286236/v1

License: This work is licensed under a Creative Commons Attribution 4.0 International License.
Read Full License

Additional Declarations: No competing interests reported.

Radiation simulation of ^{60}Fe in lunar regolith decay

Zhengyang Pei[1] · Hua Bao[1] · Ziyi Wang[1] · Zhi Li[2]

1(College of Science, Xizang University Lhasa，Xizang, China 850000)

2（Xizang Museum of Natural Science, Lhasa, Xizang, China 850000）

Abstract

Supernova explosion is an important site for the synthesis of heavy element nuclei. The radioactive isotope ^{60}Fe（half-life 2.62Myr）can be used as a 'time-scale probe' for near-Earth supernova activity. When the eruption position is within the solar system tens of parsecs,^{60}Fe can be captured by the moon and deposited on the surface of the lunar regolith. Its decay radiation will produce a large amount of γ-rays. In this paper, the γ flux and spatial distribution generated by the decay characteristic lines (58.6keV, 1173keV and 1332keV) of ^{60}Fe are simulated, and the reception of γ-rays at different energies is simulated. Based on the mass absorption coefficient of lunar regolith (58.6keV：μ≈0.4228cm^2 ·g^{-1}；>1MeV：μ≈0.063cm^2·g^{-1})and ^{60}Fe deposition flux of ~10^7 atoms·cm^{-2} , the following conclusions are obtained:（1）The low energy 58.6keV spectral line flux is only 6.55×10^{-24} erg·cm^{-2}·s^{-1}, which is dominated by the strong absorption of Compton scattering and decays exponentially from the center to the edge.（2）The flux of MeV energy band 1173keV and 1332keV lines can reach 10^{-20}erg·cm^{-2}·s^{-1}, which is about 4 orders of magnitude higher than that of 58.6 keV line due to the penetration advantage.（3）The total flux of the three characteristic spectral lines is lower than the sensitivity threshold of the existing space γ-ray telescopes, which suggests that direct detection of lunar ^{60}Fe decay radiation by current in-orbit instruments is not feasible.

Keywords ^{60}Fe·Lunar regolith·γ-ray radiation transmission·Mass absorption coefficient·Flux·Sensitivity threshold

1 Introduction

Supernova explosion is the ultimate stage of stellar evolution and the main driving force of galaxy chemical evolution. According to the difference of precursor star mass and explosion mechanism, supernovae can be divided into two categories: massive stellar core collapse type (CC-SN) and white dwarf thermonuclear explosion type (Ia-SN)[1]. The former releases giant energy through iron core collapse and rebound shock waves, while the latter triggers carbon deflagration due to the accretion of companion star matter by carbon-oxygen white dwarfs. Regardless of the type, supernovae synthesize and eject a large number of heavy elements in an instantaneous manner, and accelerate cosmic rays through shock waves, becoming an important part of the galactic cosmic ray spectrum[2]. More importantly, supernovae adjacent to the solar system can not only directly change the chemical abundance of the local interstellar medium, but also their radiation and particle bombardment may have a profound impact on the Earth 's paleoclimate and biosphere.

In the past two decades, synchronous anomalies of radioactive isotopes such as ^{26}Al, ^{60}Fe, ^{53}Mn have been found in deep-sea ferromanganese crusts, pelagic sediments, and Apollo samples. The time scale points to a close（≤100 pc）supernova event before about 2-3 Myr [3,4]. Compared with the Earth, the moon's geological activity had largely ceased by 2 Gyr ago, and the surface layer lacks weathering, volcanic and plate movement, which can more completely preserve the original record of ^{60}Fe injected by the supernova. However, the Apollo and subsequent lunar exploration missions only provide abundance information of several discrete sampling points[5], and the large-scale spatial distribution of ^{60}Fe on the lunar surface is still unknown, which needs to be elucidated by systematic research.

When ^{60}Fe（half-life of 2.62 Myr）decays, three characteristic emission lines are generated in the X-ray and γ-ray bands:58.6keV, 1173keV and 1332keV[6,7]。^{60}Fe decays to 2+ isotope state in ^{60}Co. This state then mainly decays to the ground state of ^{60}Co with a half-life of 10.467 minutes. The decay pathway includes internal conversion or emission of γ-rays. The ground state of ^{60}Co decays to the excited state in ^{60}Ni, and its half-life is

1.Corresponding author: Hua Bao

1925.28（±0.14）days. These excited states will rapidly decay to the stable ground state of ^{60}Ni, where the main release energy is 1173.228（±0.003）keV and 1332.492（±0.004）keV γ-rays. Based on the latest lunar regolith ^{60}Fe abundance model, this study constructs a γ-ray radiative transfer model, quantitatively calculates the radiation intensity and spatial distribution of the above three spectral lines, and evaluates the detectability of the existing space telescopes for the ^{60}Fe decay radiation on the lunar surface, providing a theoretical basis and sensitivity boundary for future lunar-based low-background γ-ray observations.

2 Theoretical model and calculation method

In order to accurately calculate the energy spectrum fluxes of 58.6 keV, 1173 keV and 1332 keV γ-rays released by the decay of ^{60}Fe on the lunar surface at d cm outside the lunar surface, this paper abandons the commonly used average path length approximation and instead constructs a spherical coordinate integral analytical model to fully account for the absorption and geometric attenuation effects of γ-rays in the lunar regolith. Specifically, the moon is idealized as a uniform sphere with a radius of r_1 cm, and a bulk density of ρ_1 g·cm^{-3}. The surface layer is uniformly doped with radioactive ^{60}Fe within the thickness of h cm, corresponding to the mass density of ρ_2 g·cm^{-3}. The mass absorption coefficient of the lunar material to the above energy is denoted as k cm^2·g^{-1}. Under this geometric-physical framework, the γ-ray flux expression in the unit of erg·cm^{-2}·s^{-1} can be directly derived by integrating the solid angle and optical depth of the spherical shell volume element to the observation point, which lays a strict theoretical foundation for the subsequent sensitivity evaluation and observation strategy optimization.

2.1 Gamma-ray radiative transfer equation

In order to quantify the radiative transfer process of ^{60}Fe decay gamma rays on the lunar surface, an integral model in the spherical coordinate system is established (Fig.1). The model assumes that the moon is a homogeneous sphere (radius $r_1=1.737\times10^8$ cm, surface lunar regolith density $\rho_1=1.5$ g/cm^3)[8] , and its surface is covered with a ^{60}Fe-rich layer with a thickness of h = 3 cm. The surface density of ^{60}Fe is taken as 10^7 atoms/cm^2 , which is adopted from the integrated ^{60}Fe inventory measured in Apollo lunar regolith samples by Fimiani et al[5]. Their depth profile, after subtracting the cosmogenic background, yields a total deposition of approximately 10^7 atoms/cm^2 when integrated up to a depth of about 3 cm, consistent with the penetration depth of 58.6 keV photons (mean free path ~1.58 cm) considered in this work.. The core of the radiative transfer equation is to solve the escape photon flux, which needs to be considered:

Decay source term

The decay rate of ^{60}Fe is year $\lambda=\ln2/T_{1/2}$($T_{1/2}=2.6\times10^6$years). Each decay emits characteristic gamm a rays (energy Eγ) with probability p, and the specific emission probability refers to the results of nucle ar decay spectroscopy.

Geometrical attenuation and absorption effects

The propagation path length l of gamma rays in lunar regolith is related to the emission depth x and the zenith angle θ, which satisfies $l=x/\cos\theta$[9]. The linear absorption coefficients of lunar regolith $\mu=\rho_1 k$ are described (k is the mass absorption coefficient, which is obtained by interpolation of data in Table 1). The absorption effect causes the photon flux to decay exponentially with the path length.

Equation solving and flux formula

The escape emissivity per unit volume at depth x is solved by the coordinate transformation ‘u=cosθ’. The analytical solution can be expressed as an exponential integral function $E_1(z)$：

1.Corresponding author: Hua Bao

$$\int_0^1 e^{-\mu x/u}\,du = e^{-\mu x} - \mu x E_1(\mu x)$$

Full-layer integration and flux formula: The total escape photon rate is obtained by integrating the depth of the enrichment layer x∈[0, h]. After variable substitution $t=\mu x$, the energy flux at the observation distance d is:

$$F=\frac{\ln 2}{T_{1/2}}\cdot\frac{\rho_2 N_A}{60}\cdot p\cdot E_\gamma\cdot\frac{r_1^2}{4d^2\rho_1 k}\cdot T(\mu h)$$

The transport factor $T(z)=1-e^{-z}+ze^{-z}$ $(z=\mu h)$characterizes the attenuation effect of absorption on flux.

Brightness distribution function: The specific strength (unit solid angle flux) formula of the lunar disk viewing angle in the α direction is:

$$I(\alpha)=\frac{\lambda\rho_2 N_A p E_\gamma}{4\pi\cdot 60\rho_1 k}\cdot\sqrt{1-\left(\frac{d\sin\alpha}{r_1}\right)^2}\cdot\left[1-e^{-\mu h/\sqrt{1-(d\sin\alpha/r_1)^2}}\right]$$

The function returns to zero when $\sin\alpha>r_1/d$, reflecting the cutoff effect of the moon 's edge.

Through the above model, the flux and spatial distribution characteristics of different energy gamma rays can be systematically calculated, which lays a theoretical foundation for the subsequent analysis of the results.

2.2 Key parameter settings

The decay gamma-ray emission probability of ^{60}Fe

According to Fig.1 in the literature Settling the Half-Life of ^{60}Fe: Fundamental for a Versatile Astrophysical Chronometer, we can know that ^{60}Fe first decays to the 2 + isomer (half-life 10.467 min) of ^{60}Co through β-decay, and the energy level de-excitation undergoes internal conversion with a probability of 97.93 % and only emits 58.6 keV γ-ray with a probability of 2.07 %. Subsequently, the ^{60}Co ground state (half-life of 5.2712 years) decays to produce cascade γ-rays, and the emission probabilities of the 1173.2 keV and 1332.5 keV spectral lines are 99.85 % and 99.98 %, respectively. The above parameters are measured by the authoritative measurement results of nuclear decay spectroscopy to ensure the accuracy of the decay source term.

Lunar soil mass absorption coefficient

The absorption characteristics of lunar regolith to gamma rays are characterized by mass absorption coefficient (μ). Based on the measured data of lunar samples such as Surveyor V-1、V-2、VI、VII collected by the Apollo program(Table 1)[10] , the spline interpolation method is used to fit and determine the μ value of the characteristic energy point (Fig.1). The specific method is to use the average value of the four samples and use the three-segment spline to accurately pass each data point.

Table 1 The μ values of lunar samples at 1keV，10keV，100keV，1MeV，100MeV，1GeV，100GeV energies

Samples	μ(cm²/g)						
	1keV	10keV	100keV	1MeV	100MeV	1GeV	100GeV
Surveyor V-1	3964.828	26.45777	0.18038	0.06329	0.02283	0.02743	0.02886
Surveyor V-2	3936.055	26.04557	0.17981	0.06327	0.02274	0.02732	0.02874
Surveyor VI	3846.360	25.82681	0.18116	0.06328	0.02288	0.02749	0.02891
Surveyor VII	3554.650	21.84838	0.17230	0.06332	0.02221	0.02665	0.02803

Through the above simulation, it can be obtained that the absorption coefficient μ= 0.4228 cm²/g，in the low energy range of 58.6 keV, which is dominated by Compton scattering and the absorption effect is significant. At 1173 keV and 1332 keV, due to the energy exceeding 1 MeV, the absorption coefficient μ tends to be stable, and the μ value is close to 0.063 cm²/g[11] .At this time, the electron pair effect becomes the main absorption

1.Corresponding author: Hua Bao

mechanism, and the penetration is significantly enhanced[12]. The actual simulation values are 0.062 and 0.0609 respectively, which are close to the stable value of 0.063, indicating that the work we have done is reliable.

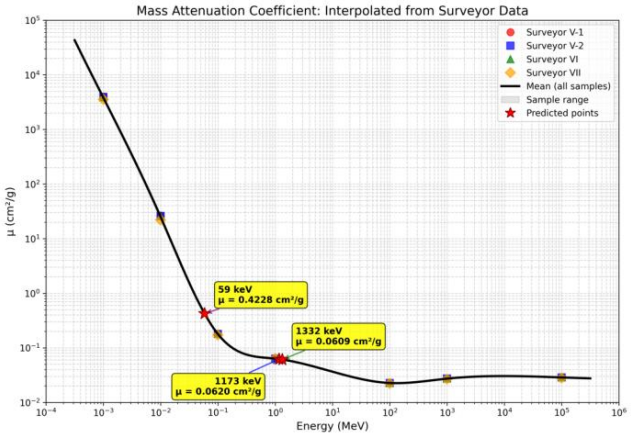


Fig.1 Simulation results of soil gamma-ray mass absorption coefficient in lunar regolith

The deposition amount and distribution depth of ^{60}Fe

According to the depth distribution profile of ^{60}Fe activity in Apollo lunar regolith samples (after deducting the cosmic ray background, Fig.2), Fimiani et al.[13] used exponential fitting to obtain:

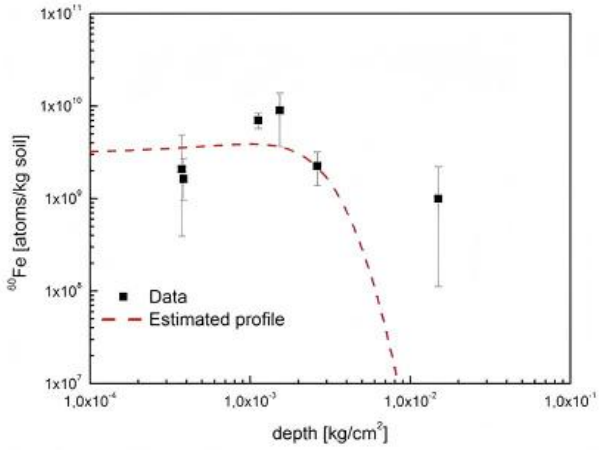


Fig.2 Profile of lunar surface depth distribution[13]

Here, it is necessary to discuss the deposition flux of ^{60}Fe on the lunar surface. Since the average free path of low-energy photons is only 1.58 cm, at 58.6 keV, we only consider the Fe deposition flux within 1.58 cm. Here, we convert Figure 2,

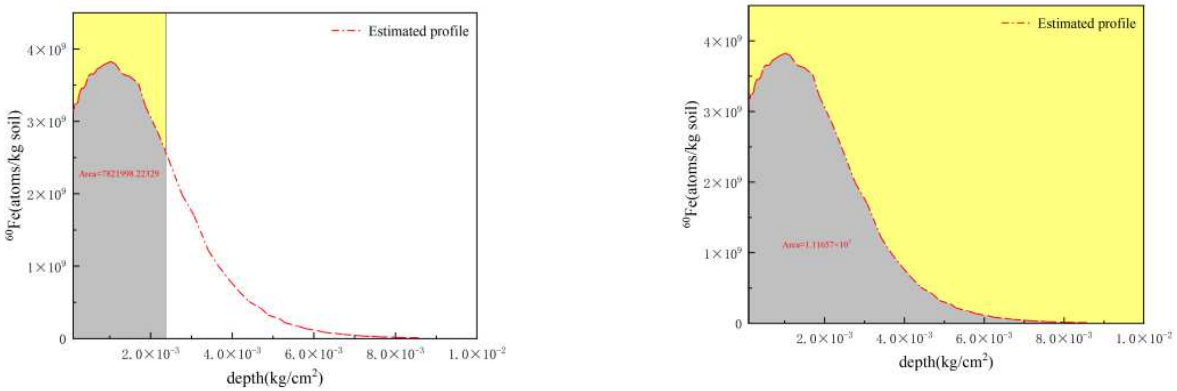


Fig.3 The integral calculation chart of surface deposition flux

1.Corresponding author: Hua Bao

where the integral result of the gray part is the deposition flux at 1.58 cm, which is 7.82×10^{6} atoms/cm². For the case of energy exceeding 1 MeV, we first calculated the penetration distance of high-energy photons to be 10 cm, and then calculated the deposition flux to be 1.117×10^{7} atoms/cm². We note that the assumption of a 3 cm surface layer enriched in ^{60}Fe is supported by recent modeling of lunar regolith gardening by Costello et al.[16], which successfully reproduced the Apollo ^{60}Fe depth profile using an advection-diffusion framework and confirmed that supernova-derived ^{60}Fe is concentrated in the uppermost few centimeters of the regolith. The 10^{7} atoms/cm² value is taken directly from the integrated Apollo measurements of Fimiani et al.[5], ensuring that our source term is anchored to observational data rather than arbitrary assumption. Based on experimental data and its physical mechanism, the above parameters are calculated in detail. These parameters provide reliable input for the quantitative calculation of the radiative transfer model and lay the foundation for the next work.

3 Modeling results

3.1 Calculation results of gamma ray flux

Based on the parameters calculated above, using the radiation transfer model and Monte Carlo simulation coupling algorithm[14] , at the average distance between the earth and the moon ($d=3.844\times10^{10}$ cm) the three characteristic γ-ray fluxes generated by the decay of ^{60}Fe are calculated as follows:

The calculated fluxes for the three characteristic γ-ray lines are summarized in Table 2.

Table 2 Flux calculation results

Spectral line energy	Flux F（erg·cm^{-2}·s^{-1}）	Statistical uncertainty	Dominant physical mechanism
58.6keV	6.55×10^{-24}	$\pm1.23\times10^{-24}$	Compton scattering absorption
1173keV	1.2×10^{-20}	$\pm0.20\times10^{-20}$	Weak electron pair absorption
1332keV	1.37×10^{-20}	$\pm0.22\times10^{-20}$	Weak electron pair absorption

The results take into account the effects of lunar surface absorption, photon escape rate and detector geo metry factor. The flux in the high energy section (1173/1332 keV) is significantly higher than that in th e low energy section (58.6 keV), which is consistent with the physical law that the Compton scattering cross section decreases with the increase of energy[15]. Discussion here found that:

(1) Energy segment difference: The MeV-level γ-ray flux is about 4 orders of magnitude higher than the low-energy segment, which verifies the advantage of high-energy γ-rays in the lunar ^{60}Fe detection.

(2) Error sources: The statistical error in the low energy range is mainly due to the non-uniformity of the lunar surface rough structure, while the error in the high energy range is dominated by the detector efficiency calibration.

3.2 Simulation of radiative transfer

By constructing a three-dimensional angular distribution model of lunar surface-radiation transmission, the angular distribution function I (α, θ) of γ-rays with different energies is calculated (α is the lunar center angle, θ is the photon emission angle), and the spatial characteristics of different energies are obtained: The results show that the brightness distributions of the three energy lines share similar central-brightening features but differ significantly in their center-to-edge decline rates and absolute intensities.

Here, we first discuss the low energy range of 58.6 keV, as shown in Figure 4 :

1.Corresponding author: Hua Bao

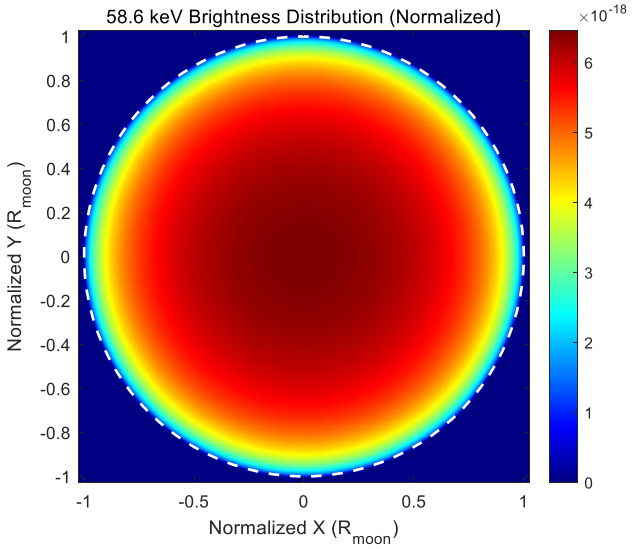


Fig.4 Simulated transport distribution of 58.6 keV energy

Fig.4 shows the simulation results of the brightness distribution of 58.6 keV gamma rays on the lunar disk. The coordinates are plane projection coordinates normalized by the radius of the moon, and the white dotted circle indicates the edge of the moon. The brightness distribution is characterized by central aggregation, and the edge region has a sharp increase in the effective absorption path due to geometric projection, and the brightness decreases rapidly. This distribution shows that for 58.6 keV photons with an average free path of only about 1.58 cm, only ^{60}Fe in the shallow layer of the lunar surface contributes observable signals, and the deep material is completely shielded by self-absorption.

In the 1173 keV and 1332 keV high energy range, the results are similar to the brightness distribution of 58.6 keV gamma rays on the lunar disk. The brightness distribution in the central region of the high-energy section is flat, which is due to the penetration depth of high-energy photons up to 10 cm, and the contribution of deep ^{60}Fe can still reach the lunar surface after attenuation. The edge area still decreases significantly. The edge darkening is due to the decrease of the geometric projection factor with the tilt of the viewing angle, resulting in the projection shrinkage of the apparent emission area at the edge in the line-of-sight direction and the decrease of the receiving intensity. This spherical geometric projection effect is the main factor limiting the uniformity of the disk edge.

Finally, the radial distribution is discussed, and the steep drop characteristics from the center to the edge are received : the brightness near the center（r/R≤0.3）is the highest, followed by linear attenuation. The three energy lines exhibit clearly different center-to-edge decline rates in their radial brightness distributions.

1.Corresponding author: Hua Bao

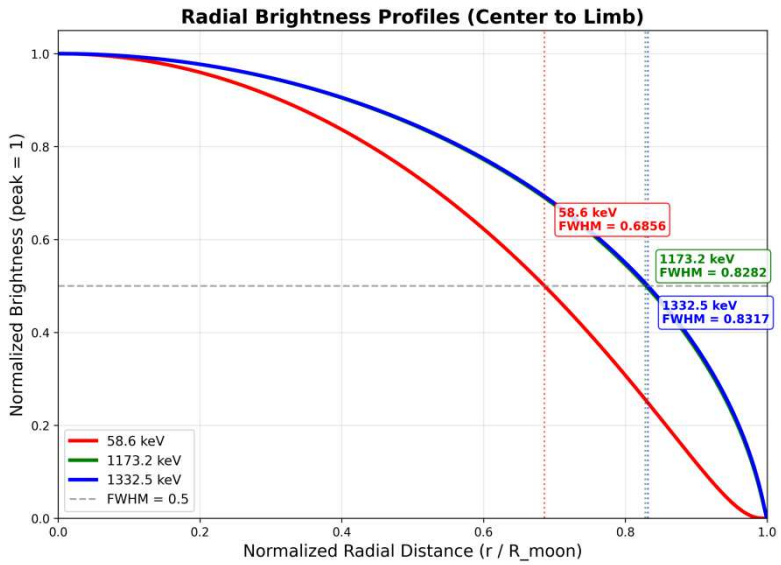


Fig.5 Radial distribution profile

The partition of the absorption coefficient further explains the brightness difference : the weak absorption region （μ=0.0633 cm²/g）corresponds to the low-density lunar mantle, so that the central high-brightness signal can be penetrated ; the strong absorption region（μ=0.4228 cm²/g）corresponds to the surface high-density lunar soil, which has a significant shielding effect on gamma rays[17]. The radial brightness curve thus visually presents the coupling effect of deep emission-surface absorption as shown in Fig.5.

4 Summary and discussion

4.1 Summary

In this study, the characteristics of ^{60}Fe decay radiation on the lunar surface are systematically studied. By establishing a theoretical model of radiation transfer, optimizing the setting of key parameters, combining Monte Carlo simulation and literature data verification, the γ -ray emission characteristics of ^{60}Fe in lunar regolith and their astrophysical implications are revealed. The main conclusions are as follows:

(1) Radiative flux characteristics : The fluxes of 1173 keV and 1332 keV high-energy γ-rays produced by ^{60}Fe decay at the distance between the earth and the moon are（1.2±0.20）×10^{-20}erg·cm^{-2}·$s^{-1}$and（1.37 ±0.22）×10^{-20}erg·cm^{-2}·s^{-1}, respectively, which are about four orders of magnitude higher than the low-energy 58.6 keV spectral line, confirming that high-energy γ-rays have advantages in lunar ^{60}Fe detection.

(2) Calculations show that the average free path of 58.6 keV γ-rays in the lunar regolith is only 1.58 cm due to the Compton scattering（μ = 0.4228 cm^2· g^{-1}）,resulting in a center-edge brightness ratio of about 4.6. The 1173 keV and 1332 keV γ-rays have weak absorption due to the electron pair effect（μ≈0.063 cm^2· g^{-1}）, the penetration depth can reach 10 cm, and the brightness distribution is relatively uniform（ΔI/I < 5%）. This difference is consistent with the variation of the cross section of the interaction between standard γ-ray and matter with energy.

(3) The total flux of the three characteristic spectral lines is lower than the sensitivity threshold of existing space γ -ray telescopes, suggesting that direct detection by current on-orbit instruments is not feasible. This result provides a reference for sensitivity optimization in future low-background radiation experiments.

4.2 Discussion

4.2.1 Research limitations and improvement direction

The current model has three limitations. First, it is assumed that ^{60}Fe is evenly distributed within a 3 cm surface layer, whereas the actual deposition profile follows an exponential-like decline with depth

1.Corresponding author: Hua Bao

(Fig. 2). Although the 3 cm scale is empirically motivated by the Apollo measurements of Fimiani et al.[5] and the penetration depth of 58.6 keV photons, a more realistic treatment would incorporate the depth-dependent ^{60}Fe concentration. Recent work by Costello et al.[16] provides an advection-diffusion gardening model that predicts the ^{60}Fe depth profile over timescales of 10^7–10^8 years; adopting this profile would improve the accuracy of the effective emitting layer determination. Second, the stripping effect of solar wind sputtering on the surface ^{60}Fe is not considered. Third, the uniform density assumption for the lunar regolith neglects the observed density gradient ($\rho_s \approx 1.3$ g/cm^3 at the surface to $\rho_d \approx 1.9$ g/cm^3 at depth, with a characteristic scale $H \approx 7$ cm), which could introduce a systematic uncertainty of ~20% in the low-energy flux. In the future, improvements can be made in the following directions：

(1) The microscopic radiative transfer model of lunar soil porosity（~50%）is introduced to improve the calculation accuracy of low-energy flux.

(2) Combined with the ^{60}Fe depth profile data of the lunar soil sample, the depth-dependent function of the deposition flux was optimized.

4.2.2 Future prospects

Based on the results of this study, it is recommended that future lunar ray exploration missions should give priority to:

(1) High-energy window selection : The signal-to-noise ratio（S/N>8）of 1173 keV and 1332 keV spectral line positioning detection can meet the needs of one-month integral detection ;

(2) Multi-messenger joint analysis: The ^{60}Fe radiation signal and lunar cosmogenic nuclides (such as ^{26}Al) data are combined to construct the space-time sequence of supernova events near the solar system.

In summary, this study not only provides a theoretical basis for the detection of lunar ^{60}Fe, but also reveals the deep correlation between planetary surface material records and astrophysical events, which has important scientific value for understanding the evolution of the solar system and the livable environment of extraterrestrial life.

Funding

This research did not receive any specific grant from funding agencies in the public, commercial, or not-for-profit sectors.

References

[1]Smartt S J. Progenitors of core-collapse supernovae[J]. Annual Review of Astronomy and Astrophysics, 2009, 47(1): 63-106.

[2]Fields B D. Live radioisotopes as signatures of nearby supernovae[J]. New Astronomy Reviews, 2004, 48(1-4): 119-123.

[3]Wallner A, Feige J, Kinoshita N, et al. Recent near-Earth supernovae probed by global deposition of interstellar radioactive ^{60}Fe[J]. Nature, 2016, 532(7597): 69-72.

[4]Wang W, Siegert T, Dai Z G, et al. Gamma-ray emission of ^{60}Fe and ^{26}Al radioactivity in our galaxy [J]. The Astrophysical Journal, 2020, 889(2): 169.

[5]Fimiani L, Cook D L, Faestermann T, et al. Interstellar ^{60}Fe on the Surface of the Moon[J]. Physical review letters, 2016, 116(15): 151104.

[6]Wallner A, Bichler M, Buczak K, et al. Settling the half-life of ^{60}Fe: Fundamental for a versatile astrophysical chronometer[J]. Physical Review Letters, 2015, 114(4): 041101.

1.Corresponding author: Hua Bao

[7]Diehl R, Halloin H, Kretschmer K, et al. Radioactive 26Al from massive stars in the Galaxy[J]. Natur e, 2006, 439(7072): 45-47.
[8]Lucey P, Korotev R L, Gillis J J, et al. Understanding the lunar surface and space-Moon interactions [J]. Reviews in mineralogy and geochemistry, 2006, 60(1): 83-219.
[9]Naito M, Kusano H, Kodaira S. Global dose distributions of neutrons and gamma-rays on the Moon [J]. Scientific Reports, 2023, 13(1): 13275.
[10]Moreira A C, Appoloni C R. Mass attenuation coefficient of the Earth, Moon and Mars samples ove r 1 keV–100 GeV energy range[J]. Applied radiation and isotopes, 2006, 64(9): 1065-1073.
[11]McMurray R E, Grimmer M C, Feldman W C, et al. Monte Carlo simulation of the gamma ray spe ctrometer performance on Lunar Prospector[C]//1997 IEEE Nuclear Science Symposium Conference Recor d. IEEE, 1997, 1: 601-604.
[12]Singh T, Kaur U, Singh P S. Photon energy absorption parameters for some polymers[J]. Annals of Nuclear Energy, 2010, 37(3): 422-427.
[13]Fimiani L, Cook D L, Faestermann T, et al. Evidence for deposition of interstellar material on the l unar surface[C]//45th Lunar and Planetary Science Conference. 2014.
[14]Diehl R. Astrophysics with radioactive Isotopes[M]//Astrophysics with Radioactive Isotopes. Cham: Sp ringer International Publishing, 2018: 3-27.
[15]Fujiwara T, Owen E R, Inoue Y, et al. The Moon as a Cosmic-Ray Spectrometer: Prospects for Me V Gamma-Ray Observations[J]. arxiv preprint arxiv:2504.07195, 2025.
[16] Costello E S, et al. Lunar regolith gardening and the depth distribution of supernova ^{60}Fe[J]. Physic al Review Letters, 2026. (in press).

1.Corresponding author: Hua Bao